The Research Council of Norway (NFR)

NORSAR

NORSAR Scientific Report No. 2-96/97

Semiannual Technical Summary

1 October 1996 – 31 March 1997

Kjeller, May 1997

APPROVED FOR PUBLIC RELEASE, DISTRIBUTION UNLIMITED

7.4 Threshold Magnitudes

Introduction

This note is intended to explain some of the basic principles and assumptions behind the calculation of threshold magnitudes, such that the reader can get an understanding of how this method can be used as part of a CTBT verification system. In addition, we will outline the current status on the development of the threshold monitoring system, as well as the plans for further improvements and extensions.

Definition of station and network magnitude thresholds

Several studies have confirmed that global observations of body-wave magnitude m_b are normally distributed with a standard deviation of about 0.4 m_b units (a.o., Veith and Clawson, 1972; Ringdal, 1976). This is one of the basic assumptions behind the calculation of m_b magnitude thresholds.

If we look for a hypothetical event at a given location and origin time, and consider a "noise situation" at a given station i, i.e., that there are no phase detections at the predicted phase arrival time of the hypothetical event, we can calculate a so-called "noise magnitude" a_i.

If a hypothetical event of magnitude **m** really was present, it would have phase magnitudes m_i normally distributed around **m**, and for station i we would know that $m_i \leq a_i$. This is used in the statistical derivation of the single station and network magnitude thresholds, and for details we refer to Ringdal and Kværna (1989, 1992).

Using the formulas developed for calculation of network magnitude thresholds we find that if we e.g., have **one single** station observation with a "noise magnitude" of m_b 4.0 for a hypothetical event at a given location and origin time, we can say (with 90 per cent confidence) that a hypothetical event would need to have an m_b less than 4.52. If we, on the other hand, had **two** station observations each with a "noise magnitude" of m_b 4.0, we can say (with 90 per cent confidence) that a hypothetical event would need to have an m_b less than 4.20. In a similar way, all network station observations of "noise magnitude" can be combined to place an upper m_b limit on a hypothetical event occurring at a given location and origin time.

By repeating the calculation of network magnitude thresholds in origin time steps, we obtain a so-called threshold trace for a given geographical location. It has been shown in several NORSAR reports and papers that such a threshold trace can be effectively used to conduct a site-specific threshold monitoring of interesting areas like the Novaya Zemlya and Lop Nor nuclear test sites.

By gridding the Earth into discrete target areas, we can compute threshold traces for each separate target area, and then interpolate to create global or regional maps of magnitude thresholds. From inspecting these maps we can get an instant picture of the monitoring capability of the network, as well as being able to identify regions and time intervals with particularly high magnitude thresholds. The primary causes of such increases would be signals and coda from large events and/or station outages.

What happens to the magnitude thresholds when an event occurs?

In cases when signals are observed from an event occurring in the target area, we would for the detecting stations have $m_i = a_i$ and **not** $m_i \leq a_i$, which was one of the basic assumptions behind the statistics of the network threshold calculations. In such a case our magnitude threshold will be biased low, and the bias will generally increase with the magnitude of the event. In such a situation, the correct approach would be to use the maximum-likelihood formalism of Ringdal (1976), taking into account both the detecting and non-detecting stations of the network. But this will require that we have available both the event locations from the standard network processing, as well as knowledge of which stations had detections on the beams used for threshold calculations.

As a preliminary solution to this problem, we have chosen to provide information on the detected events (from the AELs or the REBs) together with the threshold maps and threshold traces, such that the user can be aware that the actual threshold magnitudes are biased low around the origin time and location of the events.

Strictly speaking, the magnitude threshold calculations should also handle situations when an event occurred in the target area, without being detected by the processing algorithms. The reason for this could be SNRs below the detection thresholds or too few stations detecting the event. In this case the bias in threshold magnitudes will be negligible, and the conservativeness used in our parametrization should be able to accommodate such situations.

As an example, a 3 station event in Finland with a maximum-likelihood m_b of 2.71 resulted in a 90% magnitude threshold of 2.66 using data from the full Alpha network. This event was, however, detected by the processing algorithms, so the difference between the estimated m_b and the 90% magnitude threshold is probably higher that what can be expected for non-detected events. In any case, the bias effect resulting from ignoring the detection information is very small for such low-magnitude events.

Tuning of the Alpha network

In order to obtain useful and reliable results from the Threshold Monitoring (TM) system, we have during the last months spent most of our resources on the tuning of the stations in the Alpha network. From analysis of a fairly extensive event database of 20-60 events per station, we have for each of the stations derived the following parameters:

- The frequency bands for filtering of the beams used to monitor targets in the different distance regimes (local, regional or teleseismic).
- The relations between the manual A/T measurements in the 0.8-4.5 Hz band and the STA values of the filtered beams. This has been done to ensure compatibility between the PIDC magnitude measurements and the magnitude thresholds provided by the TM system.
- For the arrays, we have derived beam sets that ensure complete coverage of the entire Earth, using the constraint that the maximum allowable beamloss caused by mis-steering of the beams was 3 dB. In addition, we have derived expected values for the signal loss by beamforming.

The derivation of frequency bands for filtering of the beams was a quite difficult task, as it often involved balancing of two conflicting demands. The first was to ensure that for the events analyzed there was generally a good correspondence between the STA values of the filtered beams and the manual A/T measurements in the 0.8-4.5 Hz band. On the other hand, we also wanted to obtain low magnitude thresholds during regular noise conditions.

In order to verify the quality of our tuning, we have for about 15 events compared the PIDC station magnitudes with the station magnitudes derived from the STA traces of the TM system. The agreement seems to be remarkably good, but because of the small data set available at NORSAR, we have not yet been able to compile any comprehensive statistics.

An example is given in Table 1, for an event located southwest of Africa. For all Alpha stations outside the distance interval 97-125 degrees, we have computed station magnitudes from the STA traces of the TM system. Except for the station LPAZ, we find a very close agreement between the PIDC station magnitudes and the STA magnitudes. We suspect that the PIDC station magnitude at LPAZ actually is a measurement of the strong noise field leaking into the 0.8-4.5 Hz filter band. The dominant period of 1.6 seconds indicates this. For LPAZ, we have in the teleseismic regime decided to use a bandpass filter between 1.0 and 4.5 Hz for calculation of STA station magnitudes. In this particular case, this filter ensured that we actually measured the signal. At the bottom of Table 1 we show a comparison between the PIDC network magnitude, the PIDC network magnitude of the Alpha stations within 97 degrees, the STA based network magnitude of the Alpha stations within 97 degrees, and the STA based network magnitude of all Alpha stations outside the distance interval 97-125 degrees. A significant feature is the lower standard deviation of the STA based station magnitudes.

The reason for not having analyzed a larger data set is that we need to transfer all raw data of the Alpha network to NORSAR prior to the analysis. But as soon as the new DFX beam recipes are operating on the Testbed, we would be able to compile such a statistics on a much larger data set. Our goal would then be to investigate whether the PIDC and the TM system provide on the average the same station and network magnitudes, and determine to which extent TM magnitudes are useful to supplement PIDC magnitudes.

Network capability and magnitude thresholds

As another indirect test of the quality of the tuned TM parameters we have computed a simplified three-station detection capability map of the Alpha network using data from a time interval without any reported events. Our TM capability map has been computed by choosing the **third lowest** of the station "noise magnitudes", and then adding 0.7 m_b units to accommodate an SNR of 5.0 required for phase detection. The TM capability for 1997-058:20.08 is shown in Fig. 7.4.1, where the black circles symbolize operating Alpha stations and the red circles symbolize Alpha stations without available data. This capability map show striking similarities with the simulated 90% detection threshold for the GSETT-3 network presented in Fig. 5.2.a of CD report no. 1423 (4 September 1996), although there are a few minor differences between the configurations of the GSETT-3 network and the operating Alpha network of February 27, 1997. Thus, the very simple "third lowest TM magnitude" approach provides an excellent approximation to the standard 3-station 90% capability maps.

It should also be emphasized that the capability map of the GSETT-3 network is derived from statistical models of signal and noise characteristics, whereas the TM capability is derived from actually observed noise data. In this way, the TM approach is able to immediately accommodate variations in detection capability caused by "unusual" conditions like station outages, large earthquakes or aftershock sequences, which may cause the network capability to deteriorate for hours.

In contrast to the "capability maps" discussed above, the standard TM maps include no assumptions on the SNR threshold required for detection or the minimum number of stations required to generate an event hypothesis. Instead, the observed "seismic field" is used to place an upper limit to the magnitude of possibly hidden events. Fig. 7.4.2 shows the 90% magnitude threshold for the same origin time instant as used in the capability map of Fig. 7.4.1. While the capability map of Fig. 7.4.1 tells us that for most of the region north of 30^0 N our processing algorithms will be unable to detect events below m_b 3.5, the threshold map of Fig. 7.4.2 tells us that if there was an event in this region it would need to have a magnitude below 3.0. For the areas close to some of the stations, the magnitude thresholds are even below 2.5.

In somewhat simplified terms, we could say that the TM approach is able to "monitor" an area at an m_b level 0.5 units lower than the conventional "detection based" approach.

In order to illustrate the effect of the occurrence of a large earthquake, we have estimated the three-station detection capability and the magnitude thresholds for a time instant 9 minutes after the origin time of a M_S 7.2 earthquake located in Pakistan. The capability map of Fig. 7.4.3 tells us that except for parts of Australia and parts of north and south America, the detection threshold is above 4.5 for the entire Earth. For parts of Asia and Africa, the threshold even exceeds 5.0.

When turning to the magnitude thresholds of Fig. 7.4.4, we find significantly smaller numbers. The usefulness of the threshold map is illustrated by the fact that while we could not be certain to detect a magnitude 5 event in parts of Asia and Africa, the threshold map tells us that a hypothetical event in these regions could not have had a magnitude significantly above 4. For most parts of the world, we find the upper magnitude limits to be about 1 m_b unit lower than the three-station detection capability in this case. So the "gain" by applying the TM technique is even greater than during noise conditions.

Usage of magnitude thresholds and capability maps in CTBT monitoring

It should be evident from the discussions above that both the magnitude threshold maps and the detection capability maps could be useful supplements in the monitoring of a CTBT. While the capability maps provide the lowest event magnitude the processing system is likely to detect, the magnitude threshold maps put an upper limit to the size of a possibly hidden event.

An application of the capability maps and the threshold maps would be to provide continuous confirmation and quantification of the monitoring capability of regions of interest to the international community. In addition, these maps would also provide an instantaneous warning and quantification of a reduced monitoring capability during station outages or high-noise intervals.

Another scenarios for the use of the results from the TM system would be investigation of time intervals for which questions have been raised regarding possible non-compliance with the treaty. By going back to the magnitude threshold maps for a given region and time interval, we could by selecting the pointwise maxima of the magnitude threshold maps for the given time period, get a useful overview of the maximum size of a hypothetical event in the region during this time period. This could be helpful to decide if further investigation would be needed. Along the same lines we could display the threshold trace for given target areas. If this trace shows an increase that is **not** caused by any known event, and at the same time exceed a magnitude threshold of interest, it might be meaningful to continue the investigation. E.g., our one-month monitoring experiment of the Novaya Zemlya test site (Kværna, 1992) showed that from inspection of the threshold traces, we were able to exclude 99.7% of the total time from search for signals from possible events at the test site. The remaining 0.3% of the time contained threshold increases that could be explained by signals from detected interfering events.

If the magnitude thresholds for a given region show increased values during a particular time interval, we would like to know the reason why so happened. Signals from events located outside the region, station outages or increased noise levels at some stations are usually the main causes. By looking into the event bulletins and the station performance reports it should be possible to explain the majority of the threshold increases. But if threshold peaks remain unexplained, we should start to look more closely for events in the target region. This could be done by optimized manual data analysis of the stations known to have the best capability for the given target region, and/or by requesting and analyzing additional data.

Status and plans for TM development for the PIDC

Our most immediate task for the TM development for the PIDC is to install the tuned processing recipes for the Alpha network on the Testbed. Following this installation it will be necessary to monitor the performance of the processing system both with regard to operational reliability, processing load and quality of the results. After this test is completed, hopefully within 3-4 weeks after the installation on the Testbed, we would be ready to consider the transfer of the TM processing system to the operational pipeline.

During the last months we have also been working with the development of TM products to be distributed from the PIDC. So far we have developed a program for creation of maps with pointwise maxima of the magnitude thresholds for each half-hour time interval. We will continue the discussions with the PIDC staff on which and how the TM products can be presented within the framework of PIDC services.

Another remaining task is the development of procedures for archiving of TM results. We have not yet decided how to do this, but it seems reasonable to store both the basic STA traces for each of the Alpha stations, as well as the maps provided through the PIDC services. But before deciding on the archiving procedures, we have to define the contexts in which the archived data are to be used. By contexts we mean situations like focused investigation of particular areas for previous time intervals, or re-assessment of the monitoring capability using additional data from the Beta stations or non-IMS networks.

We would also like to emphasize that we still consider the TM system to be experimental and under development, and that we have concentrated on producing high quality results from the basic processing algorithms. As soon as we have confirmed the quality of these computations, we will be ready to go ahead with the development of functions and products that can be useful for monitoring compliance with the CTBT. Our main focus will be on the usage of threshold and capability maps, as well as the threshold traces for each of the target areas.

Future applications

For the future, we have in mind several interesting applications of data from the TM system that could be useful in the CTBT context.

E.g., we showed in the previous chapters that there seems to be a very good agreement between the PIDC magnitudes and the STA based magnitudes from the TM system. It would therefore be interesting to investigate if the usage of STA based magnitudes will provide any improvement to the network m_b estimates. By combining the STA traces with a detector, it will also be quite straightforward to implement procedures for **automatic** maximum likelihood m_b estimation, which again will help to reduce the m_b bias problem for smaller events.

Another interesting application is threshold monitoring of surface waves. In principle, such processing should be feasible using the already existing processing modules, but some studies on filter settings, STA lengths and the usage of surface magnitude correction tables would be needed. The upper limit M_s calculation could be applied to extend the functionality of discriminants like M_s/m_b. For small explosions, surface waves frequently are too weak to be observed at any station of the recording network. Obtaining reliable upper bound on M_s in such cases would expand the range of usefulness of this discriminant. In practice, an "upper bound" for single station measurements has often been given as the "noise magnitude" at that station, i.e., the M_s value that corresponds to the actually observed noise level at the expected time of the Rayleigh arrival. The threshold monitoring procedure will include this as a special case of a more general network formulation.

Once we have at hand reliable **automatic** procedures for both magnitude estimation and upper limit calculation of m_b and M_s, it might provide useful to investigate the usage of these data for **automatic** event screening via M_s/m_b.

As a final comment, we still believe that the best monitoring performance is achieved through an optimized site-specific monitoring, incorporating region-specific calibration information like travel time, slowness and magnitude anomalies, and optimal bandpass filters for assessment of magnitude thresholds. Such high-quality monitoring has already been demonstrated for the Novaya Zemlya and the Lop Nor test sites, using data from the Scandinavian arrays. By integrating the output from the optimized site-specific threshold monitoring with the results from "traditional" data analysis of detected signals we would utilize the resources of the monitoring network in a new tool that might enable a very high continuous automatic monitoring capability.

T. Kværna

References

CD/1423 (1996): Report of the Ad Hoc Group of Scientific Experts to the Conference of Disarmament on the GSETT-3 experiment and its relevance to the seismic component of the Comprehensive Nuclear Test-Ban Treaty International Monitoring System

Kværna, T. (1992): Continuous seismic threshold of the northern Novaya Zemlya test site; long-term operational characteristics, *PL-TR-92-2118, Phillips Laboratory, Hanscom Air Force Base, Mass., USA.*

Ringdal, F. (1976): Maximum- likelihood estimation of seismic magnitude, *Bull. Seism. Soc. Am.*, 66, 789-802.

Ringdal, F. and T. Kværna (1989): A multi-channel approach to real time network detection, location, threshold monitoring. *Bull. Seism. Soc. Am.*, 79, 1927-1940.

Ringdal, F. and T. Kværna (1992): Continuous seismic threshold monitoring, *Geophys. J. Int.*, 111, 505-514.

Veith, K. F. and G. E. Clawson (1972). Magnitude from short-period P-wave data, *Bull. Seism. Soc. Am.*, 62,435-452.

EVENT 963562

Date	Time	Latitude	Longitude	Depth	Ndef	Nsta	Gap	Mag1	N
	rms	OT_Error	Smajor	Sminor	Az	Err	mdist	Mdist	Err	
1997/02/27	20:22:54.6	-52.3900	16.7500	0.0 f	22	19	114	mb 4.6	12
	1.03	+- 0.65	31.2	25.4	44		20.21	165.00	+-0.4	

SOUTHWEST OF AFRICA

Sta	Dist	EvAz	Phase	Time	Def	SNR	Amp	Per	Mag1	MagTM
SUR	20.21	10.0	P	20:27:31.4	T	6.4	51.3	1.08	mb 4.8	
TSUM	33.12	1.4	P	20:29:32.6	T	5.4	7.3	1.08	mb 4.5	
VNDA	48.56	170.4	P	20:31:39.3	T	4.2	11.8	1.00	mb 4.7	4.57
BGCA	57.36	2.0	P	20:32:44.5	T	11.9	3.4	0.97	mb 4.3	4.16
PLCA	57.62	244.0	P	20:32:47.1	T	3.1	2.3	0.90	mb 4.1	4.29
PLCA	57.62	244.0	PcP	20:33:40.7	T	3.2	2.2	0.83		
CPUP	60.03	265.0	P	20:33:04.0	T	4.6	2.2	0.40	mb 4.5	4.56
DBIC	61.65	335.4	P	20:33:14.2	T	4.3	5.0	0.83	mb 4.5	4.41
BDFB	62.39	280.4	P	20:33:20.0	T	13.0	14.2	0.98	mb 4.9	4.86
LPAZ	74.17	263.8	P	20:34:34.5	T	13.1	50.8	1.60	mb 5.3	4.47
LPAZ	74.17	263.8	PcP	20:34:47.0	T	5.9	5.4	1.10		
STKA	83.26	135.3	P	20:35:23.5	T	10.0	8.1	0.95	mb 4.8	4.49
ASAR	86.62	125.2	P	20:35:40.3	T	34.5	12.3	1.10	mb 5.0	4.85
WRA	89.95	123.5	P	20:35:55.7	T	8.4	1.1	0.80	mb 4.2	3.95
SCHQ	127.22	313.8	PKP	20:42:00.7	T	7.2	4.0	0.73		4.77
TXAR	131.00	266.2	PKP	20:42:08.4	T	10.9	2.1	1.00		4.39
PDAR	143.30	276.7	PKP	20:42:27.4	T	22.6	2.3	0.65		4.55
MNV	145.99	264.0	PKPbc	20:42:35.0	T	23.1	21.9	1.00		4.84
MBC	150.80	340.1	PKPbc	20:42:46.7	T	15.2	7.4	0.98		
YKA	152.60	310.8	PKP	20:42:43.8		9.5	0.9	1.04		
YKA	152.60	310.8	PKPbc	20:42:52.0	T	4.7	2.1	0.57		4.12
YKA	152.60	310.8	PKPab	20:43:01.2	T	4.9	0.7	0.72		
ILAR	165.00	332.2	PKPab	20:43:58.0	T	10.1	1.5	1.05		4.41

Average PIDC magnitude : 4.63, St.dev. 0.35

Average PIDC magnitude (Alpha network < 97 deg): 4.63, St.dev. 0.38
Average TM magnitude (Alpha network < 97 deg): 4.46, St.dev. 0.28

Average TM magnitude (Alpha network) : 4.49, St.dev. 0.27

Table 7.4.1. REB bulletin information for an event southwest of Africa. The PIDC magnitudes are given in the Mag1 column, whereas the STA-based TM magnitudes are given in the MagTM column. The average network m_b values and the corresponding standard deviations are given at the bottom of the table.

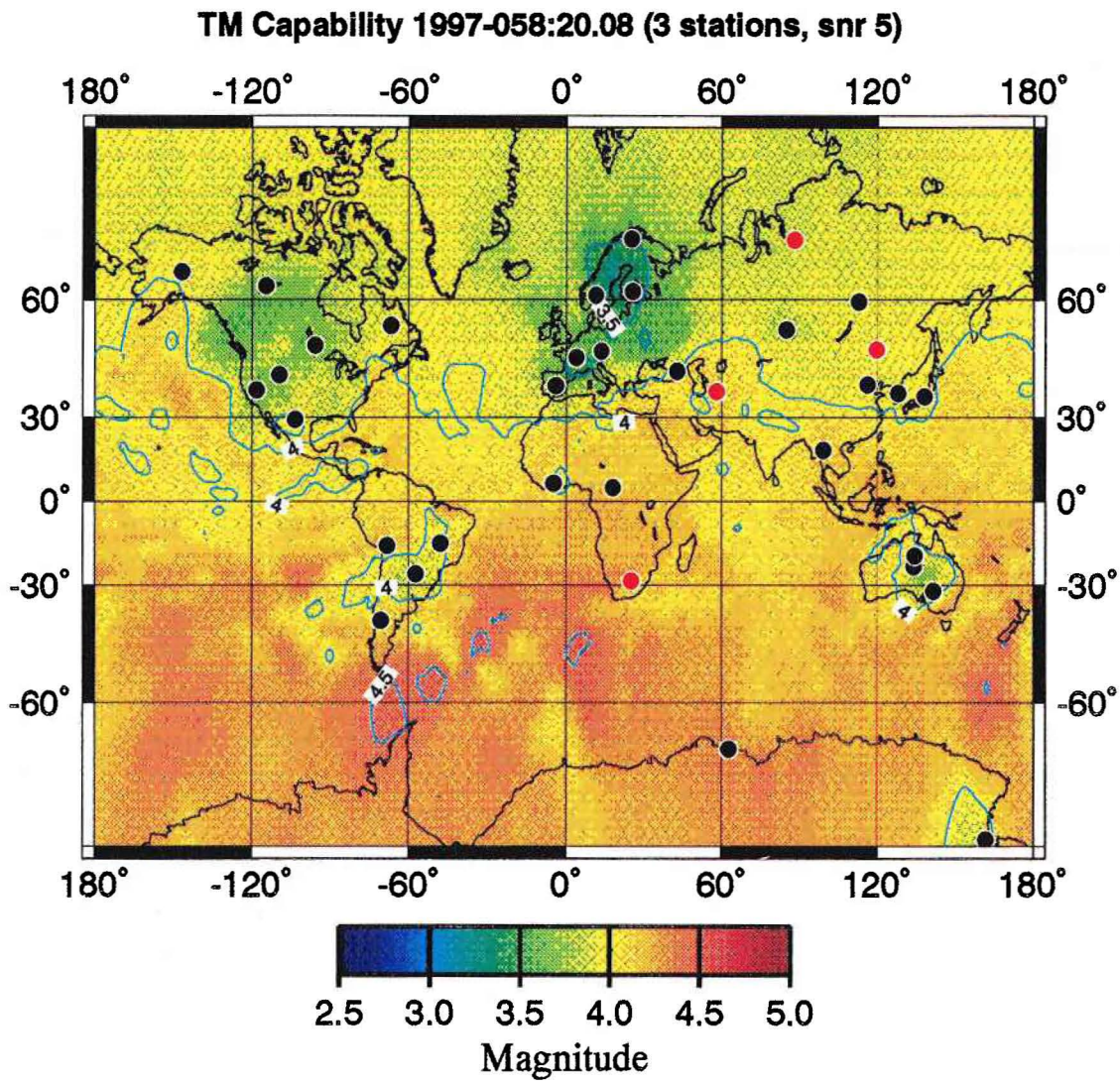

Fig. 7.4.1. Three-station detection capability map during noise conditions for the Alpha network for the time instant 1997-058:20.08. The capability map has been computed by choosing the **third lowest** *of the station "noise magnitudes", and then adding 0.7 m_b units to accommodate an SNR of 5.0 required for phase detection. The black circles symbolize operating Alpha stations and the red circles symbolize Alpha stations without available data.*

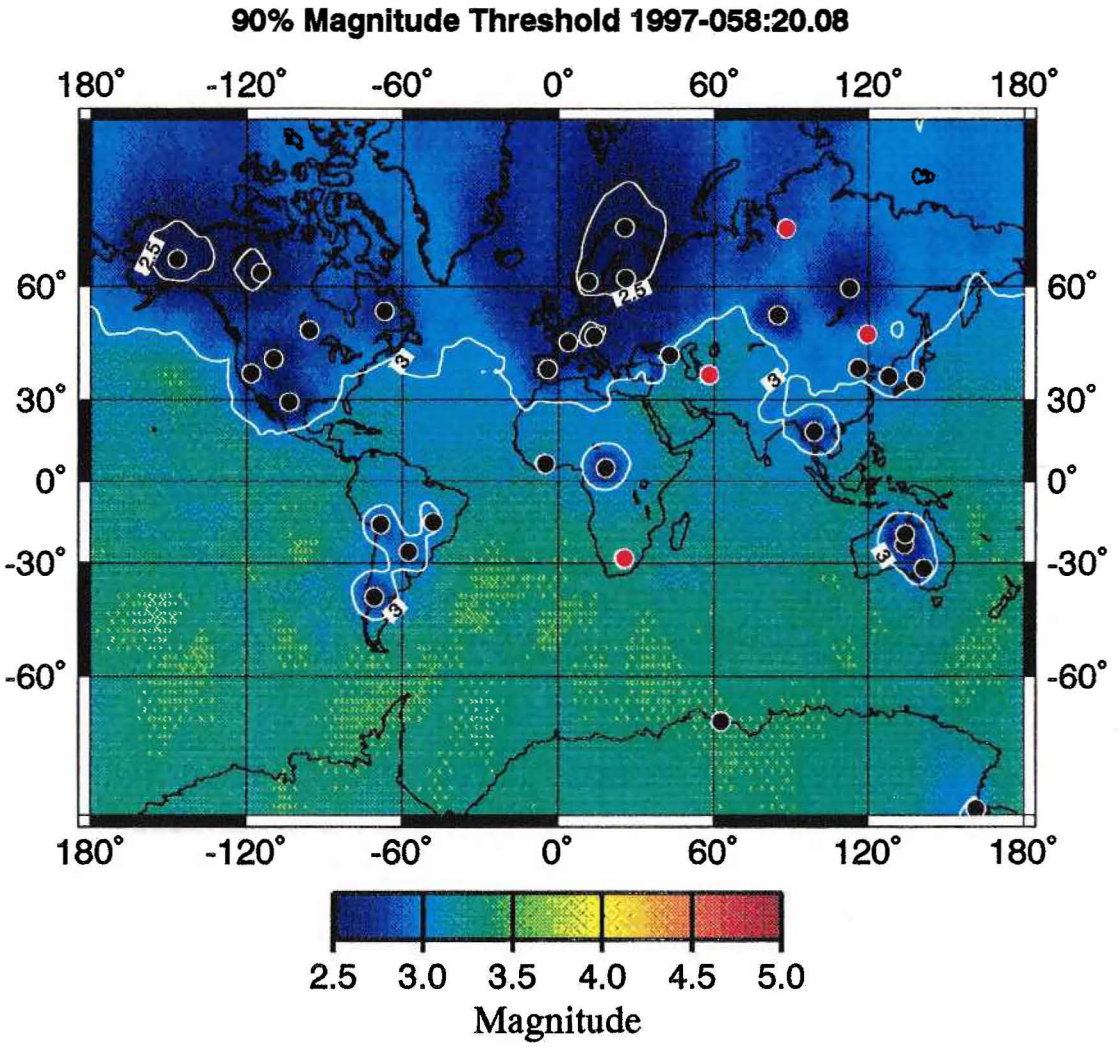

Fig. 7.4.2. 90% magnitude threshold for the same origin time instant as used in the capability map of Fig. 7.4.1.

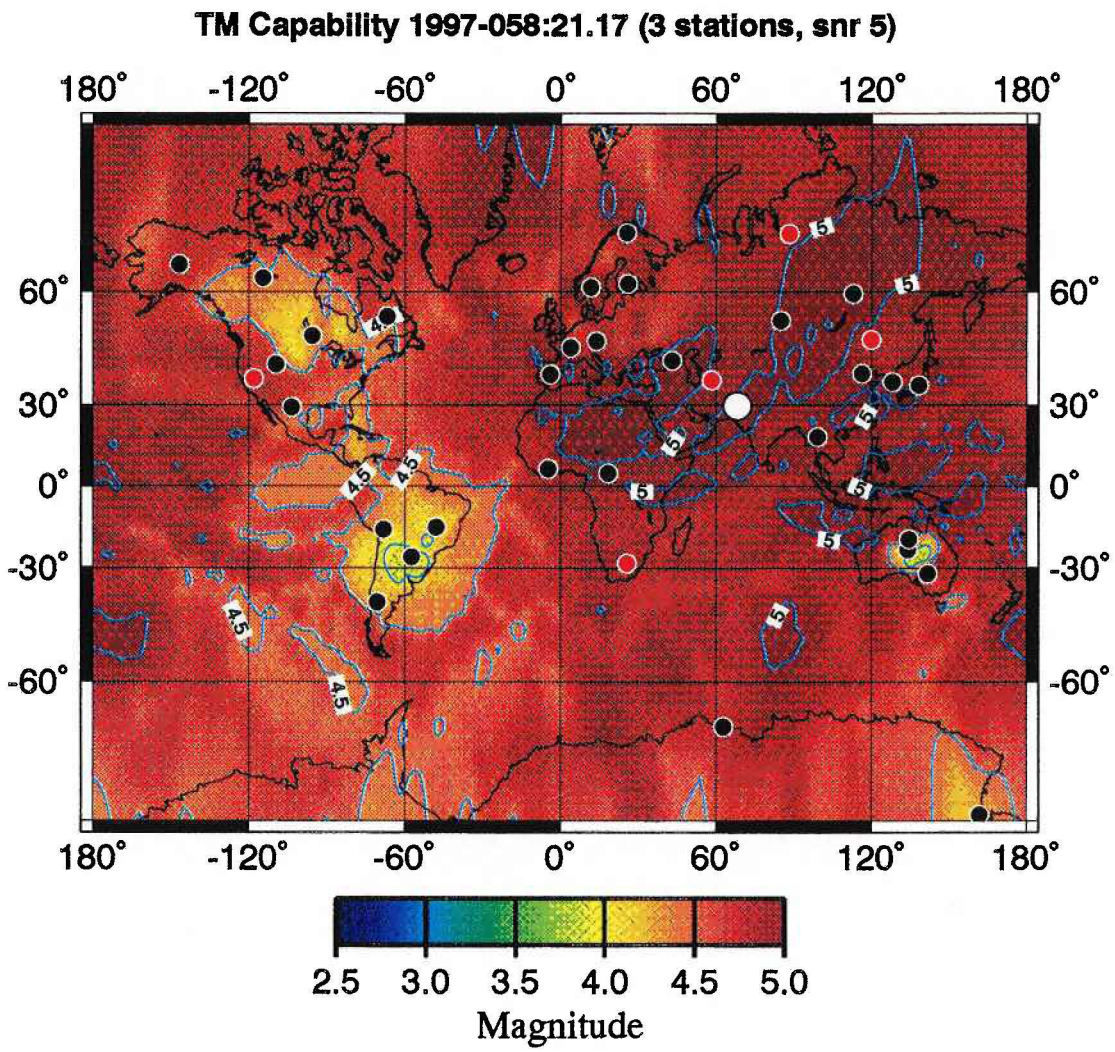

Fig. 7.4.3. Three-station detection capability 9 minutes into the coda of a M_S 7.2 earthquake located in Pakistan (white symbol). Again, the black circles symbolize operating Alpha stations and the red circles symbolize Alpha stations without available data

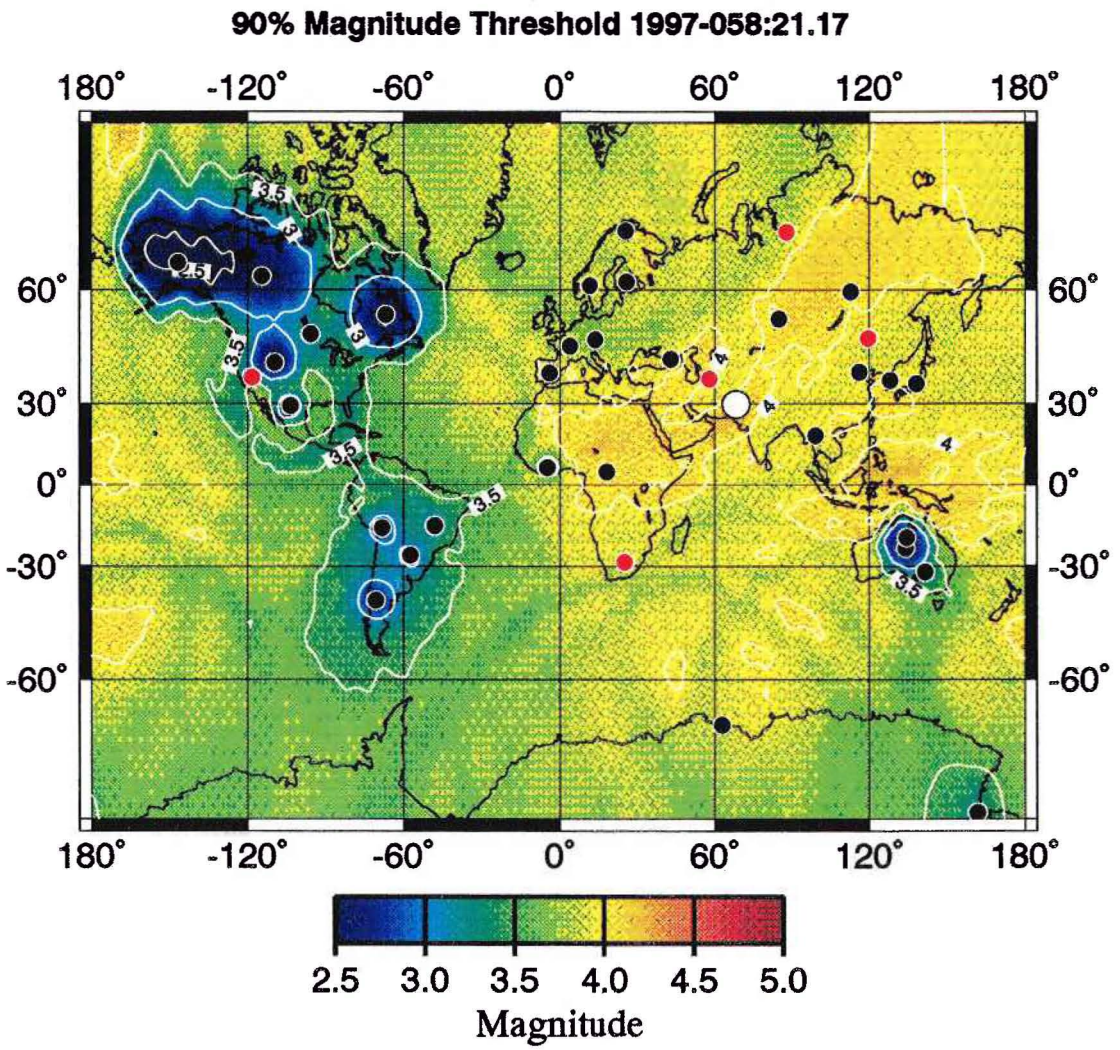

Fig. 7.4.4. 90% magnitude threshold for the same origin time instant as used in the capability map of Fig. 7.4.3.